

Percolation network in a smooth artificial potential

G. M. Gusev*

CNRS-LCMI, F-38042 Grenoble, France

and Instituto de Física de São Carlos, 13560-970, Universidade de São Paulo, SP, Brazil

U. Gennser†

CNRS-LCMI, F-38042 Grenoble, France

X. Kleber

CNRS-LCMI, F-38042 Grenoble, France

and INSA, Toulouse 31077, France

D. K. Maude

CNRS-LCMI, F-38042 Grenoble, France

J. C. Portal

CNRS-LCMI, F-38042 Grenoble, France

and INSA, Toulouse 31077, France

D. I. Lubyshev, P. Basmaji, and M. de P. A. Silva

Instituto de Física de São Carlos, 13560-970, Universidade de São Paulo, SP, Brazil

J. C. Rossi

Universidade Federal de São Carlos, São Carlos, Brazil

Yu. V. Nastaushv

Institute of Semiconductor Physics, Russian Academy of Sciences, Siberian Branch, Novosibirsk, Russia

(Received 8 December 1997)

A percolation network of the edge states in an artificial potential of a gate-controlled antidot lattice has been studied in a high magnetic field. The longitudinal resistance of the antidot lattice shows a boxlike behavior in certain ranges of the magnetic field, because of the reflection of the topmost edge state by the saddle potential between two antidots. The riser between zero and quantized resistance shows a temperature dependence due to the broadening of the percolation transition by inelastic scattering. The shift of the transition point in magnetic field with the temperature is found to originate from the mixing between Landau levels due to the inelastic scattering. It allows us to separate the exponent of the scattering mechanism and the critical exponent in the localization-delocalization transition. [S0163-1829(98)00232-X]

INTRODUCTION

The nonzero longitudinal resistance in the quantum Hall regime is currently understood in terms of percolation through the two-dimensional electron gas (2DEG) along the contours of the disordered potential. In a network model of the electron trajectories, one-dimensional transmission lines are connected by saddle points, where scattering or tunneling between the lines can occur.¹ If the electron energy E is larger than the saddle-point potential E_c , the electron is transmitted past the potential hill, whereas if $E < E_c$ the trajectories are repelled by the saddle point, and electrons move around the potential valley. However, for $E = E_c$ tunneling processes must be taken into account, as electrons can jump between different transmission lines. At this energy, it is possible for the electrons to percolate through the sample, leading to the finite resistivity risers in the transition regions between different quantum Hall plateaus. In other words, close to E_c there exists a narrow “tunneling” band of width $\Delta_t = \Gamma(l/\lambda)^2$, where Γ is the width of the Landau level, l is

the magnetic length, and λ is a correlation length of a random potential. Within this band quantum tunneling effects must be taken into account. In this case the localization length ξ_{loc} diverges as $|E - E_c|^{-\gamma}$, where $\gamma = \frac{7}{3}$.² Outside this band ($|E - E_c| > \Delta_t$) the quantum effects play no role, and percolation becomes classical. In this case the electron scatters between transmission lines, which form the percolation cluster with a characteristic length ξ_p . The size of the percolation cluster diverges according to the universal law $\xi_p \sim (E - E_c)^{-4/3}$.^{2,3} In the quantum regime the interference between electron waves is responsible for the localization. It brings an energy scale Δ_c into the problem, within which the localization can be considered in terms of the phase-breaking length. A scaling analysis of the diffusive transport⁴ shows that the transition between localized-delocalized states is determined by the condition

$$L_{\text{in}} \sim \xi_{\text{loc}}(\Delta_c), \quad (1)$$

where L_{in} is the phase-breaking length due to the inelastic scattering. The second energy scale Δ_c can be determined

from Eq. (1). Because of the existence of the two energy scales, the behavior of the system should depend on the ratio Δ_c/Δ_t .⁵ Thus, only for $\Delta_c/\Delta_t \ll 1$ and $kT \ll \Delta_t$ is relation (1) valid, and Δ_c exhibits universal scaling behavior (in accordance with the definition in Ref. 5, this is the case of a short range potential). Otherwise, the width of the conductance peak grows linearly with temperature.⁵ However, for a short-range potential, even if the universal scaling condition (1) is fulfilled, the temperature dependence of the transition region is not universal, but depends on the inelastic scattering:

$$|E - E_c| \sim T^{-\kappa}, \quad (2)$$

with $\kappa = p/\gamma$, where p is the exponent of the scattering mechanism. Different physical situations and theoretical approaches predict different temperature dependencies of the transition region: (a) $\kappa = 1/2\gamma$, if $L_{\text{in}} = (D\tau_{\text{in}})^{1/2}$, $\tau_{\text{in}} \sim T^{-1}$ for diffusive transport,⁴ (b) $\kappa = 2/\gamma$, if $\tau_{\text{in}} \sim T^{-2}$ for Landau electron-electron scattering mechanism in clean metals,^{2,6} (c) $\kappa = p/\gamma$, if $\tau_{\text{in}} \sim T^{-p}$ for electron-phonon scattering mechanism with $p = 1-4$, depending on the temperature and magnetic-field range,^{4,7} and multifractality of the electron wave function.⁷ In contrast to the case of the noninteracting electrons, a quantum percolation model with Coulomb interactions gives a dynamical scaling exponent equal to 1,⁸ which leads to (d) $\kappa = 1/\gamma$. Finally, for hopping transport in the short-range scattering case (e) $\kappa = 1/\gamma$ has been obtained.⁹ Early experiment of the temperature dependence of the transition between two Hall plateaus and the half width of the diagonal resistance ρ_{xx} demonstrated a ‘‘universal’’ exponent $\kappa = 0.42 \pm 0.04$.¹⁰ However, later it was found that κ depends on the doping level, varying from 0.4 to 0.8.¹¹ This nonuniversality of the critical exponent has been interpreted as interplay between different scattering mechanisms,⁶ or by the influence of the mobility on the electron-phonon scattering.⁷ More recently this nonuniversal behavior of κ has been explained as a transition from a short-range to a long-range potential regime. In this case $\lambda \gg 1$, so for realistic temperatures $kT \gg \Delta_t$, and the width of the conductivity peak grows linearly with T , which gives $\kappa \approx 1$ in relation (2).⁵ However, firm evidence is somewhat elusive, partly because the temperature dependence only measures the composite exponent κ , and does not separate the interaction and the percolation exponents.

The network model also implicates that the transition between different quantum Hall phases will result in a temperature-independent, universal value of the conductivity $\sigma_{xx} = e^2/2h$ at the critical percolation point.¹² In a single-electron picture this result can be traced to the fact that tunneling gives an equal probability for moving along any equipotential line connected by the saddle point, but it has also been verified in the fractional quantum Hall regime,¹³ as well as in Monte Carlo studies.¹⁴ The first correct estimation for the peak value and the ratio of two successive peaks based on the quasiclassical approach has been done in Ref. 15. However, experimentally no evidence for this universal character of the magnetoresistance has been found, and instead a large variation between different samples (even from the same wafer) has been found at low temperatures.^{10,16} In some recent theoretical studies explanations have been offered why the universality has not been observed. It has been

suggested that the interaction between edge states belonging to different Landau levels can result in an effective levitation of the energy levels.^{17,18} The temperature dependence of the interaction would then shift the percolation point, so that no temperature-independent resistance value would be observed. In order to explain the absence of any universal resistance value at very low temperatures, Ruzin, Cooper, and Halperin, have suggested that the cause may be small, macroscopic inhomogeneities in the impurity potential.¹⁹

In view of these negative experimental results, and the theoretical propositions, we have studied the transition between different quantum Hall states, using a sample with a gate-controlled array of antidots that creates a smooth, homogeneous, artificial impurity potential. The general behavior of the magnetoresistance is similar to that of a quantum point contact, or a sample with a finger gate, in that a sufficiently large gate potential can reflect the edge state belonging to the highest Landau level, leading to a quantization of both the longitudinal resistance as well as the Hall resistance. In contrast to the normal R_{xx} risers, the quantized resistance displays two percolation transitions instead of one. The onset of the R_{xx} quantization on the low magnetic-field side corresponds to the percolation threshold as the Fermi level passes the energy of the saddle points between the antidots, whereas the high-field transition is the same as that of the Hall plateau transition, when the Fermi level passes through the percolation energy for the unpatterned part of the sample. We find that the transitions to the quantized longitudinal resistance show evidence of energy levitation, which can be accounted for by looking at the derivative dR_{xx}/dB . Because the weak levitation depends on the interaction between two edge states, the present investigation seems to offer a path towards measuring p and κ (and thus γ) independently. From these measurements we conclude that electron-electron scattering is responsible for the smearing of the localization-delocalization transition.

EXPERIMENTAL DETAILS

Two types of structures were investigated. The first consists of GaAs/Al_{1-x}Ga_xAs double quantum wells (well width, 50 Å; barrier widths, 25 Å) with a 2DEG of density $n_s = 4 \times 10^{11} \text{ cm}^{-2}$ and mobility $70-100 \times 10^3 \text{ cm}^2/\text{V s}$. In these, the small well and barrier widths lead to a large separation between the symmetric and asymmetric energy levels, approximately 6 meV higher than the Fermi level in the structures ($E_F = 14.5 \text{ meV}$ above the lowest level). Hall measurements and Shubnikov-de Haas oscillations show that only the lowest, symmetric level is occupied, and the behavior of the sample is identical to the behavior of a heterojunction 2DEG. Hall bars were patterned on the samples, using conventional lithography and etching techniques. A lateral superlattice [periodicity 0.4 μm (sample A) and 0.5 μm (sample B)] containing a macroscopic number of antidots (10^5) was fabricated in the center of the device between the potentiometric probes, using electron-beam lithography to pattern the PMMA resist, which was then covered by a gold gate. The physical diameter of the antidots is 0.1 μm . The ballistic mean free path of 0.6–0.8 μm , is larger than lattice periodicity. The second type of sample was a single heterostructure with the same electron density but with higher mo-

bility ($500 \times 10^3 \text{ cm}^{-2}/\text{V s}$). This sample (C) has a disordered antidot lattice with an average periodicity of $d = 0.7 \mu\text{m}$ and a mean deviation of the antidots from the periodical position of $0.2 \mu\text{m}$. Magnetotransport measurements were carried out in the mixing chamber of a dilution fridge ($T = 50 \text{ mK}$ to 1 K), using standard low-frequency lock-in techniques at 6.7 Hz , and with an excitation current 10 nA and lower. A magnetic field $B < 15 \text{ T}$ was applied normal to the 2DEG plane.

RESULTS AND DISCUSSION

A. Resistance quantization

With zero gate bias V_g the samples reveal the usual quantum Hall effect. However, at $T = 50 \text{ mK}$, when applying a negative or positive gate voltage, the peaks in the longitudinal resistance R_{xx} broaden at the low or high magnetic-field sides, respectively, and exhibits plateaus with the resistance minima close to zero between them. Figures 1(a), 1(b), and 1(c) show the dependence of R_{xx} and R_{xy} on B for the three different voltages for sample A. The R_{xx} plateaus are quantized with the same accuracy as the quantum Hall plateaus (the relative precision in our measurements is approximately 10^{-3}). For all the observed resistance plateaus, the transition from zero to the quantized value has the same width as a width of the riser between two Hall plateaus at zero gate voltage. Increasing V_g results in a wider plateau. When measuring the resistance as a function of gate voltage at a fixed magnetic field, one quantized plateau is observed for each field (Fig. 2). The resistance starts to be quantized at $V_g > 0.1 \text{ V}$, for both positive or negative voltages, and remains unchanged, until, at high negative V_g a dramatic, approximately exponential increase in the magnetoresistance is seen. The threshold gate voltage for this increase is lower for higher magnetic fields. For $V_g < -1 \text{ V}$ the resistance plateau as well as the Shubnikov oscillations are completely smeared out.

All observed plateaus have a resistance value equal to h/Le^2 , where L is an integer specific for each plateau. The maximum value of L , which we found for the high-mobility sample, is 20 for a negative gate voltage and 24 for a positive V_g . It is possible to relate the integer L to the number of bulk Landau levels, using the equation¹⁹

$$R_{xx} = h/Le^2 = h/e^2(N - M)/NM, \quad (3)$$

if we assume that M is the number of levels transmitted through the antidot lattice. It is then found that $M = N \pm 1$ for positive and negative voltages, respectively, if spin splitting is resolved, and $M = N \pm 2$ for unresolved spin splitting. Thus, taking into account whether the spin-splitting is resolved or not, we have a situation where either all conducting channels can pass the antidot lattice (for small V_g), one channel is rejected from the lattice ($|V_g|$ sufficiently large to form a plateau), or all channels are rejected from the antidot lattice, and the sample turns into an insulator ($V_g < -1 \text{ V}$). It is not possible to observe 2,3,4, . . . channels being rejected. This is verified when sweeping the gate voltage for a fixed field.

It is possible to give a qualitative interpretation of the boxlike behavior of the resistance. For a negative gate volt-

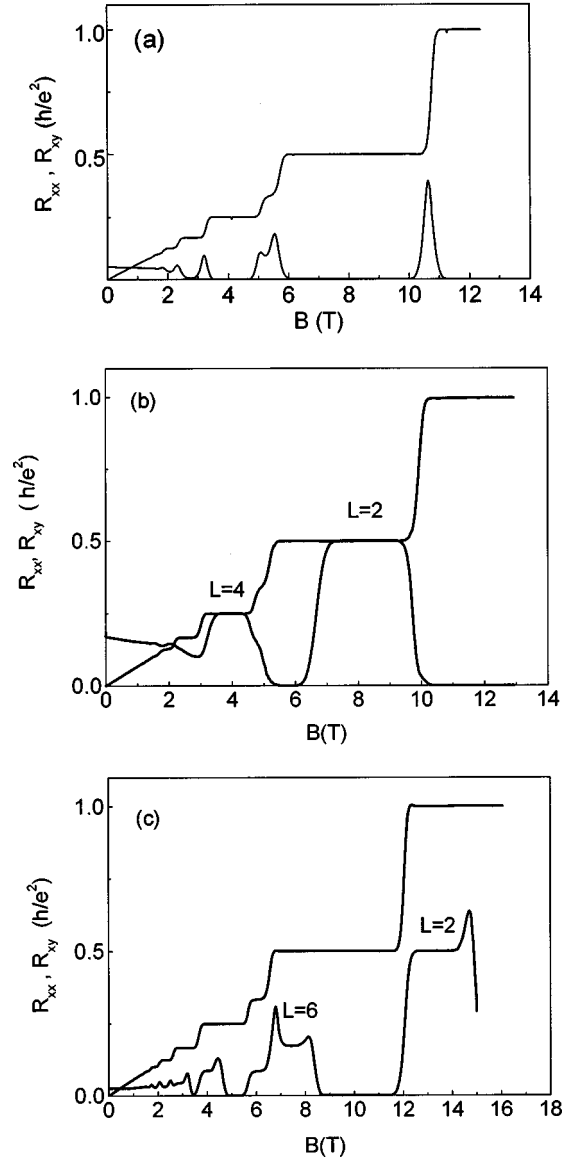


FIG. 1. Magnetoresistance and Hall resistance measured at $T = 50 \text{ mK}$ for sample A (DQW with periodicity $= 0.4 \mu\text{m}$), for three different gate voltages. (a) $V_g = 0 \text{ V}$, (b) $V_g = -0.7 \text{ V}$, (c) $V_g = +0.6 \text{ V}$.

age, all edge states may pass the saddle points if the Fermi level lies close to the first unoccupied Landau level. This is equivalent to the picture for the quantum Hall effect in macroscopic samples with a smooth disordered potential, when the Fermi level lies in between the bulk Landau levels. Because of the absence of any backscattering, longitudinal resistance is equal to zero. As the magnetic field is increased, the edge states around the antidots start to overlap, resulting in a nonzero probability of interedge state scattering. If the saddle point completely reflects the top Landau level (the outer edge state around the antidots), the situation is that considered for the quantum point contact in Ref. 20. The four-terminal resistance is determined by Eq. (3) for $M = N - 1$ transmitted channels. A positive gate voltage creates quantum dots under the gate contacts, so that the edge states near the sample border move in the same direction as the edge states around the dot, and an inverted saddle point is created. It leads to a situation similar to that of the antidot

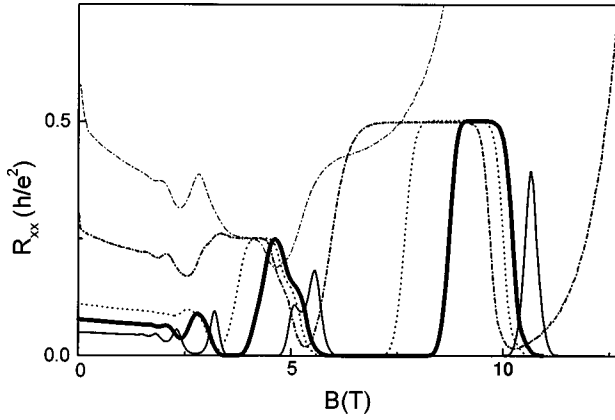


FIG. 2. Magnetoresistance for sample A, for a series of different gate voltages, $V_g = 0$ (narrow line), -0.3 V (thick line), -0.5 V (dots), -0.75 V (thick dashes), and -1 V (narrow dashes), measured at $T = 100$ mK.

lattice. With no scattering between states, R_{xx} is equal to zero. This time a decrease of the magnetic field leads to overlapping between the states and a strong mixing through the inverted saddle points near the sample border. This situation has been considered by Haug *et al.* for the case of a single thick barrier covering a macroscopic sample.²¹ They find that for the positive voltage $R_{xx} = h/e^2 (M - N)/NM$, where M is the number of channels under the gated region. Here, if the saddle points reflect one Landau level inside of the dot lattice, an additional state surrounds the lattice. Thus, $M = N + 1$, in agreement with the experimental observations.

Because the topmost Landau level with an increase of B passes the situation from an almost transparent to a nontransparent saddle point, we can use this fact to compare experimental results with a network model.¹ As predicted in Ref. 1, the percolation threshold is equivalent to a network where the transmission coefficients of each saddle point is equal to $\frac{1}{2}$. Thus, in the present case, percolation occurs when

$$E_F - \hbar\omega_c(n + \frac{1}{2}) - \frac{1}{2}g\mu B = eV_0, \quad (4)$$

where E_F is the Fermi energy at zero field, $\hbar\omega_c$ is the Landau energy gap, V_0 is a potential barrier between antidots, and $g\mu B$ is the spin splitting. The situation can be compared to that of a normal 2DEG, where V_0 is instead given by the random impurity potential with a zero average value, so that the percolation transition is exactly coincident with the center of the Landau level. In the case where the levels are spin-split one has to take into account that the positions of the levels in a strong magnetic field do not reflect the separation of the levels but their degeneracy, and the percolation transition occurs when $\hbar B/e = n_s$. The energy separation between the two last (spin resolved) is $g\mu B$. Thus, because the degeneracy of the spin-split levels is a factor of 2 smaller, the percolation field B_c is two times larger than for the last spin-unresolved levels as can be seen in Fig. 2.

B. Percolation transition

To study the influence of the inelastic processes on the percolation transition we have measured the T dependence of the longitudinal resistance in the range of the magnetic field where a boxlike behavior is seen. Figure 3 shows R_{xx} in the

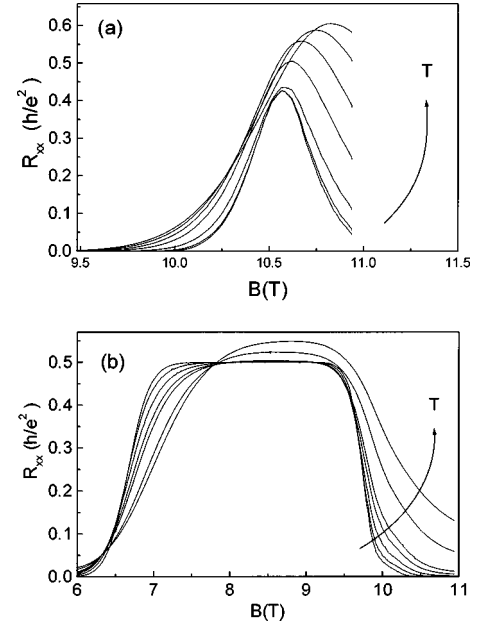


FIG. 3. R_{xx} as a function of magnetic field of sample A, for different temperatures $T = 100$ mK to 1 K. (a) $V_g = 0$ V. (b) $V_g = -0.7$ V.

region of the transition between the second and last Landau levels at $V_g = 0$ (a) and $V_g = -0.7$ V (b). As seen from Fig. 3(a) the peak of the resistance at zero gate voltage does not assume a universal value as predicted by theory,^{2,12} but depends on the temperature and shifts to a higher field. The plateau in R_{xx} at $V_g = -0.7$ V [Fig. 3(b)] remains quantized within the accuracy of the measurement for $T \sim 300$ mK. At higher temperatures it takes on a more rounded shape, with the peak resistance higher than the quantized value, which also shifts to higher B . The temperature range for which the plateau disappears, 300–800 mK, is much lower than the temperature range for which the quantum Hall effect vanishes in these samples, indicating a different mechanism. The transition regions from zero to the quantized resistance on both the high magnetic-field and low magnetic-field sides gets narrower for lower temperature. We should emphasize that there is no T -independent points in either the high- or low-field side of the transition region, contrary to the predictions for a percolation network. As mentioned above, because the transmission coefficient for the topmost Landau level passes from a value of 0 to 1, at some magnetic field it is equal to $\frac{1}{2}$, at which point a network is formed. For an ideal square antidot lattice the resistance at this field should be $R_{xx} = h/4e^2$. In the rectangular lattice employed in the experiments the resistance is expected to be $R_{xx} \approx 0.3h/e^2$, in addition to the broadening of any broadening of the transition point.

As will be discussed further on, the absence of the signature of the percolation point may be due to scattering events. In order to recover the percolation point, an analogy with the quantum Hall effect in a normal sample (without antidots) is made. It has been demonstrated that the maximum of the resistance riser occurs for the same magnetic field as the maximum of the slope dR_{xy}/dB .^{10,4} In the present situation, the longitudinal resistance plays the same role as does normally the Hall resistance, attaining a finite quantized value

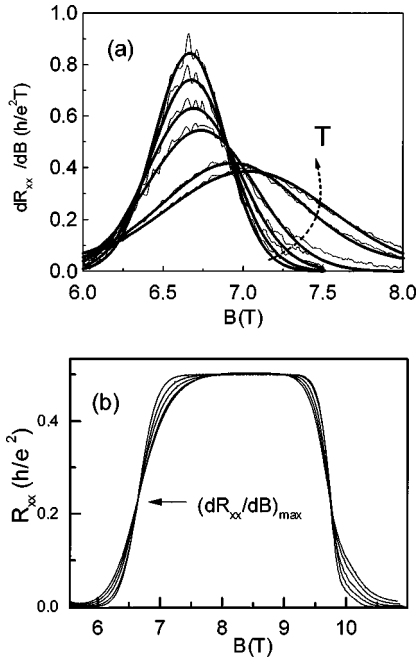


FIG. 4. (a) dR_{xx}/dB vs B for sample *A* and for different temperatures, $T=100$ mK to 1 K. The thick solid lines are Gaussian fits to the curves. (b) “Renormalized” R_{xx} vs B for $T=100$ –500 mK. The renormalization process is described in the text. The point of dR_{xx}/dB_{\max} as found from (a) is marked in the figure with an arrow.

due to the transmission coefficients being exactly one or zero for the different Landau levels. We therefore suggest that the maximum of the slope dR_{xx}/dB occurs at the percolation point. Figure 4(a) shows dR_{xx}/dB as a function of B , calculated numerically for the curves shown in Fig. 4(b). All curves have been fitted by a Gaussian to determine the maximum of dR_{xx}/dB . It is seen that the maximum is shifted to higher B for higher temperatures. It occurs for a resistance value close to the universal value $0.25h/e^2$. It is now possible to shift the curves, so that the maximum occurs at the same magnetic field (chosen as the field of the maximum of dR_{xx}/dB at 50 mK). The result of this shift is shown in Fig. 4(b), where, as a result of this renormalization, a T -independent point is now recovered at the low magnetic-field side [curves at higher temperature with peaks higher than the quantized value also cross low-field transition at the same point, if the amplitude is normalized to the quantized value, but to avoid this double renormalization, they are not shown in Fig. 4(b)]. We believe that the T -independent point constructed with this procedure reflects the percolation transition of the network formed by the edge states in the antidot potential. With the same procedure a T -independent point is also recovered for different gate voltages, with R_{\max} varying slightly between 0.3 and $0.22h/e^2$.

The magnetic-field shift (or energy shift) of the saddle point for increasing temperature can be explained by the increase of the scattering between electrons moving along percolation lines belonging to the highest Landau level ($N=1$) and the $N=2$ electrons rotating along closed loops around the potential hills (antidots). This shift due to Landau-level mixing of delocalized states, dubbed “weak levitation,” has been predicted recently.^{17,18} The effective

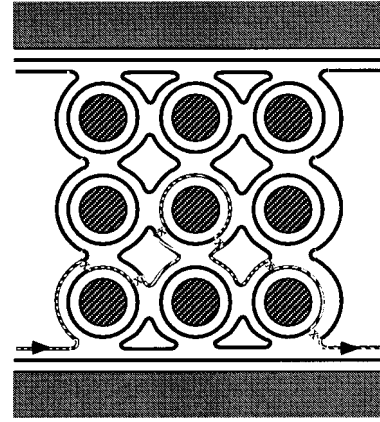


FIG. 5. Schematic illustration of the current paths through the antidot lattice. Two edge states are marked with solid lines. A possible electron path through the lattice is marked with a dashed line, where scattering events are indicated by a cross.

change of the saddle barrier potential originates from the possibility for electrons to scatter through closed loops, thus bypassing the barrier (Fig. 5). The sign of the deviation depends on the topology of the network. In the present case there are $N=1$ delocalized and $N=2$ localized states, which, according to the model, produce a downward shift of the barrier,¹⁷ in agreement with our observation. In simple terms, the scattering of an electron to an internal trajectory rotating around the antidots decreases the probability of scattering through the saddle point to the other border of the sample. To compensate this scattering, it is necessary to increase the magnetic field, and therefore the percolation threshold is shifted to the higher field. It seems reasonable that this deviation of the barrier is easier to see in the present lattice of hills than in a conventional Hall bar without antidots, where scattering by impurities is dominant. In a smooth impurity potential close to the percolation transition there can be semiclassical electron orbits around both hills and valleys, pulling the delocalized states in opposite ways, and resulting in a smaller shift than for the antidot lattice. This may be the case of the resistance risers for $V_g=0$ [Fig. 3(a), see also Ref. 10], which are shifted towards higher B with temperature; however, because the value of maximum resistance also increases, it is not possible to draw any firm conclusions whether this shift is connected with “levitation” effects.

The weak levitation model gives the shift of the saddle-point height approximately as $\delta E \sim \alpha^2 \gamma$, where α^2 is the coupling constant between two Landau levels, and γ is the characteristic parameter of the saddle point potential in a high magnetic field.¹⁷ Figure 6(a) shows the experimental shift of the last plateau with temperature for different values of gate voltage. The strong temperature dependence of the shift can be interpreted as the temperature dependence of the coupling constant α^2 . Inelastic electron scattering mechanisms can be responsible for the transition of the electrons between different semiclassical trajectories in a high magnetic field. As was mentioned above, the change in the transmission probability (ΔT) through the saddle point is compensated by the scattering from the percolation level to the internal trajectory situated around an antidot: $\Delta T \sim \Delta \mu / \mu \sim \tau / \tau_{\text{in}}$, where μ is the chemical potential of the topmost level, and τ is the time for one electron to move along equi-

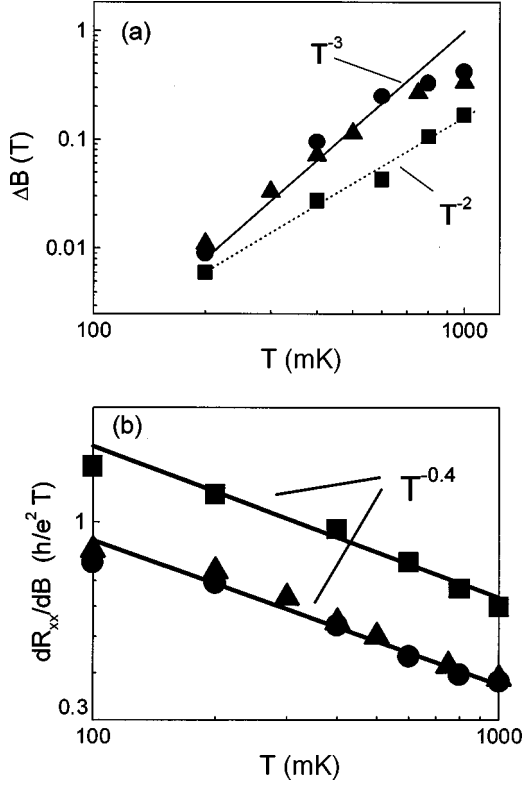


FIG. 6. (a) Experimental shift of the plateau corresponding to the $n=1 \leftrightarrow n=2$ scattering, as a function of temperature. Squares represent the shift for the gate voltage $V_g = -0.7$ V; triangles, $V_g = -0.5$ V; and circles, $V_g = -0.3$ V. The dashed and solid lines indicate T^2 and T^3 dependencies. (b) Dependence of the slope of the resistance riser in the transition point between zero and the quantized value, as a function of temperature. Squares, $V_g = -0.7$ V; triangles, $V_g = -0.5$ V; circles, $V_g = -0.3$ V.

potential line from one saddle point to another. In the present case $\tau \sim \lambda/v_{\text{dr}}$, where $v_{\text{dr}} = (c/eB)u_0/\lambda$ is the drift velocity, and u_0 and λ are the typical value and the correlation length of the smooth random potential. It should be noted that in an antidot lattice u_0 can be larger than in a system dominated by the impurity potential, where it is equal to the Landau-level broadening and of the order of 1 meV. From this equation we obtain $\Delta T \sim \delta E/\gamma \sim \tau/\tau_{\text{in}}$, so

$$\alpha^2 \sim \tau/\tau_{\text{in}}. \quad (5)$$

In order to estimate the absolute value of the deviation of the saddle barrier the parameter γ has to be known. A typical value of γ can be determined from quantized resistance measurements at zero field (the parameter of the saddle potential $\omega_y = 4.3$ meV).²² At $B = 7$ T this gives 0.5 meV. Transforming the magnetic-field shift at $T = 1$ K from the experiment at $V_g = -0.7$ V into an energy shift gives $\delta E = (\Delta B/B)g\mu B = 0.08$ meV, and hence a coupling constant in the order of 0.15. This value is smaller than unity, as prescribed by the weak levitation model. The results for the resistance plateau of $h/4e^2$ ($M=4$, $N=2$; see Fig. 1) where no shift in the percolation transition was found is also consistent with the model. For this plateau the energy gap is $h\omega_c$, and the shift in the percolation threshold $\Delta B = \delta E B/\hbar\omega_c$ is much smaller than the shift measured between the $N=1$ and $N=2$ levels, even if the energy shift is the same.

Figure 6 shows the T dependence of the percolation transition shift, which is interpreted as the temperature dependence of the coupling constant $\Delta B \sim \alpha^2 \sim 1/\tau_{\text{in}}$. In this case $\tau_{\text{in}} \sim T^{-2} - T^{-3}$. To compare the absolute value of the scattering time, the parameters $u_0 = 10$ meV, and $\lambda = 0.1 \mu\text{m}$ have been used. We estimate $\tau_{\text{in}} \approx 4.4 \times 10^{-11}$ s at $T = 1$ K. Two types of the inelastic scattering mechanism may be responsible for the mixing between levels: electron-electron ($e-e$) and electron-phonon ($e-p$) scattering. For a smooth random potential ($\lambda \gg \ell$) $e-e$ scattering has been calculated in Ref. 23 (for $T=0$) and $e-p$ scattering in Refs. 6, 7, and 24 (for $T=0$).

Let us first consider the $e-p$ interaction. It is not clear how to compare the scattering calculations of Refs. 6 and 7 with the measurements; we have instead used the results of Ref. 24. The scattering rate for the dominant piezoelectric mechanism is given by²⁴

$$1/\tau_{e-p} = A(v_{\text{dr}}/v_s)^2 (1/\hbar\Omega)^{0.86} T^{1.86}, \quad (6)$$

where v_s is the sound velocity, $\hbar\Omega = 2\pi u_0(\ell/\lambda)^2$, and A is a coefficient containing only material parameters. The temperature dependence $1/\tau_{e-p} \sim T^{-1.86}$ is close to the observed behavior. We estimate $\tau_{e-p} \approx 10^{-11}$ s, a smaller value than what is obtained in the experiments. However, this may rather be a reflection of the approximate nature of the estimation.

The $e-e$ scattering rate has been calculated for $T=0$, and is given for electrons with only a small energy ε above the Fermi energy by²³

$$1/\tau_B = (1/\tau_D)(\varepsilon/\Delta_B), \quad (7)$$

where $\Delta_B = u_0(1/\lambda)^{1/2}$ and $1/\tau_D = (e^2/\ell)^2/\Delta_B$. Naively, one can assume that for thermal electrons $\varepsilon \approx kT$, in which case $\tau_B \sim T^{-1}$, which does not agree with the experimental dependence. Furthermore, an extremely small value of $\tau_B = 5 \times 10^{-13}$ s at $T = 1$ K ($\tau_B \ll \tau \sim d/v_{\text{dr}}$) is obtained, even if it is assumed that the $e-e$ interaction is screened, and reasonable values for the parameters, $u_0 = 10$ meV and $\lambda = 0.1 \mu\text{m}$, are used. Such a small value does not agree with measurements using an electron interferometer in a high magnetic field, where an inelastic scattering time of 10^{-10} s has been obtained.²⁵ However, this naive inclusion of a temperature dependence may not be valid, and further theoretical calculations, which explicitly take into account the $T \neq 0$ case, may be necessary before a proper comparison with the experimental data can be done.

Recently, another picture of the dynamical scaling at the quantum Hall effect transition was suggested.²⁶ It has been argued that away from the transition point transport is governed by Coulomb blockade effect, because in this case 2DEG can be modeled as a dense array of the connected quantum dots. Assuming the new scale length, which is responsible for the temperature smearing of the QHE transition, authors obtained for the scattering rate the transition

$$\hbar/\tau_{\text{in}} \sim T^2/T_c, \quad T_c \sim (e^2/\varepsilon\ell)^2 \hbar/\Gamma.$$

One notes here that the temperature dependence of the scattering time due to the Coulomb interactions is close to the observed behavior, in contrast to Eq. (7). It is difficult to estimate the Coulomb interaction term in a strong magnetic

field. Naively, to use parameters for 2DEG we obtain $e^2/\epsilon l \approx 10$ meV, which is larger than $\Gamma \approx 1$ meV, and we should observe a breakdown of the integer QHE. The scattering time in this case is equal to $10^{-9}c$, smaller than the experimental value. Assuming, that the screening parameter in the strong magnetic field is different from $B=0$ and $e^2/\epsilon l \sim \Gamma \approx 1$ meV, we obtain $\tau_{in} = 10^{-11}$ s, which is close to observed value. Thus, we are not able to definitely determine the mechanism that can play an important role in the inelastic transition in strong magnetic fields and at low temperatures. Additional arguments obviously are needed to demonstrate the role of the electron-electron scattering mechanism in a strong magnetic field. Below we show these arguments.

The dominant mechanism should also be responsible for the broadening of the percolation transition in samples with antidots (here we do not consider electron scattering by electromagnetic fluctuations).^{2,27} Figure 6(b) shows the dependence of the slope of the resistance riser in the transition point between zero and the quantized value at different gate voltages. The slope of the riser can be described by Eq. (2) as for the energy of the percolation transition,^{4,10} with a critical exponent $\kappa = 0.4 \pm 0.1$, in agreement with other experiments for the transition between different Hall plateaus.¹⁰ This ‘‘universal’’ value would indicate that the potential is short range, and thus $\Delta_c/\Delta_t \ll 1$ and $kT \ll \Delta_t$, as discussed in the Introduction. The second inequality comes about since $\Delta_t \approx u_0(\ell/\lambda)^2$, and even though $\lambda \gg \ell$ (for the antidot potential) $\Delta_t \approx 1.2$ K at $B = 7$ T. On the other hand, if the magnetic length is smaller than the correlation length of the random potential, the percolation level should be broadened due to the finite width of the electron compressible stripes.²⁸ Very recently, it was argued that a charge density wave (CDW) can be a ground state of the Landau level.²⁹ In this case the narrow transition may be due to CDW pinning in a smooth potential. In this case there will only be a single electron edge state around the antidots in the percolation network, which agrees with the experiments. Using a value of $p \approx 2$, as extracted from the dependence of the saddle-point magnetic-field shift (Fig. 5) in the case of electron-phonon scattering [case (c) above], a value of $\kappa = 0.86$ is obtained, which does not agree with the direct experimental determination of κ . This apparent contradiction is resolved if the dynamic scaling exponent $z = 1$. This exponent is equal to the relevant dimensionality of the system,³⁰ and a unity value would im-

ply that the scattering time $\tau_{in} \sim L_{in}$, rather than $\tau_{in} \sim L_{in}^z$. $z = 1$ has previously been obtained in dynamic scaling experiments where the quantum Hall effect has been measured at microwave frequencies,³¹ and suggests that the carrier transport through one-dimensional edge states determine the dimensionality of the broadening mechanism. The value $z = 1$ has also been reported in a theoretical study for interacting electrons,⁸ in contrast with the results $z = 2$ for the noninteracting case. It is not clear that γ is not changed by Coulomb interactions; however, it has been suggested that the network model¹ is also valid for interacting particles.⁸

As we mentioned above, recently it was argued²⁶ that two independent processes with energy transfer—dephasing scattering [scattering rate is of order T (Ref. 27)] and inelastic scattering (scattering rate behaves as T^2)—lead to the different effects. Phase breaking time is responsible for the corrections to the critical conductivity (in our case they are negligibly small). The smearing of the percolation transition is controlled by charging effects and, consequently by inelastic $e-e$ scattering. It leads to the temperature exponent with $z = 1$ in accordance with our experiment. It arises from the fact that $\tau_{in}^{-1} \sim DL_{in}^{-2}$. In this case we can conclude that the scattering mechanism that can be responsible for the mixing of Landau levels and shift of the transition point is $e-e$ scattering. For $e-p$ scattering $\tau_{in} \sim L_{in}$ and we cannot explain the critical exponent in the localization-delocalization transition.

CONCLUSION

In summary, the present experiment has allowed for a separation of the exponent p (the temperature dependence of the inelastic scattering rate), and the exponent κ of the temperature broadening of quantum Hall transitions. The former has been obtained from the shift of the saddle point with the temperature, and the latter from the slope of the resistance delocalization transition. The measurements indicate that electron-electron scattering is responsible for the mixing between edge states around antidots and smearing of the transition.

ACKNOWLEDGMENTS

This work was supported by CNRS (France), CNPq, and FAPESP (Brazil). G.M.G. was supported by CNPq, and U.G. was supported by NFR through the HCM program.

*Present address: Instituto de Física da Universidade de São Paulo, CP 66318, 05315-970, São Paulo, SP, Brazil.

†Present address: Paul Scherrer Institute, Villigen-PSI, CH-5232, Switzerland.

¹J. T. Chalker and P. D. Coddington, *J. Phys. C* **21**, 2665 (1988).

²B. Huckestein, *Rev. Mod. Phys.* **67**, 357 (1995).

³G. V. Mil'nikov and I. M. Sokolov, *Pis'ma Zh. Eksp. Teor. Fiz.* **48**, 494 (1988) [*JETP Lett.* **48**, 536 (1988)].

⁴A. M. M. Pruisken, *Phys. Rev. Lett.* **61**, 1297 (1988).

⁵D. G. Polyakov, cond-mat/9608013 (unpublished).

⁶H. L. Zhao and S. Feng, *Phys. Rev. Lett.* **70**, 4134 (1993).

⁷T. Brandes, L. Schweitzer, and B. Kramer, *Phys. Rev. Lett.* **72**, 3582 (1994); T. Brandes, *Phys. Rev. B* **52**, 8391 (1995).

⁸D. H. Lee, Z. Wang, and S. Kivelson, *Phys. Rev. Lett.* **70**, 4130 (1993).

⁹D. G. Polyakov and B. I. Shklovskii, *Phys. Rev. Lett.* **70**, 3796 (1993).

¹⁰H. P. Wei, D. C. Tsui, M. Paalanen, and A. M. M. Pruisken, *Phys. Rev. Lett.* **61**, 1294 (1988).

¹¹S. Koch, R. J. Haug, K. von Klitzing, and K. Ploog, *Phys. Rev. B* **43**, 6828 (1991).

¹²J. T. Chalker and G. J. Daniell, *Phys. Rev. Lett.* **61**, 593 (1988).

¹³S. Kivelson, D. H. Lee, and S. C. Zhang, *Phys. Rev. B* **46**, 2223 (1992); D. B. Chklovskii and P. A. Lee, *ibid.* **48**, 18 060 (1993); A. M. Dykhne and I. M. Ruzin, *ibid.* **50**, 2369 (1994).

¹⁴Y. Huo, R. E. Hetzel, and R. N. Bhatt, *Phys. Rev. Lett.* **70**, 481 (1993).

¹⁵B. Shapiro, *Phys. Rev. B* **33**, 8447 (1988).

¹⁶J. K. Wang and V. J. Goldman, *Phys. Rev. B* **45**, 13 479 (1992); R. Willet *et al.*, *Phys. Rev. Lett.* **59**, 1776 (1987).

- ¹⁷T. V. Shahbazyan and M. E. Raikh, Phys. Rev. Lett. **75**, 304 (1995).
- ¹⁸V. Kagalovsky, B. Horovitz, and Y. Avishai, Phys. Rev. B **52**, R17 044 (1995).
- ¹⁹I. M. Ruzin, N. R. Cooper, and B. I. Halperin, Phys. Rev. B **53**, 1558 (1996).
- ²⁰C. W. J. Beenakker and H. van Houten, *Quantum Transport in Semiconductor Nanostructures* (Academic, New York, 1991), Vol 44.
- ²¹R. J. Haug, J. Kucera, P. Streda, and K. von Klitzing, Phys. Rev. B **39**, 10 892 (1989).
- ²²J. E. E. Frost, K. F. Berggren, M. Pepper, M. Grimshaw, D. A. Ritchie, A. C. Churchill, and G. A. C. Jones, Phys. Rev. B **49**, 11 500 (1994).
- ²³Y. Levinson, Phys. Rev. B **51**, 16 898 (1995).
- ²⁴S. Iordanski and Y. Levinson, Phys. Rev. B **53**, 7308 (1996).
- ²⁵X. Liu *et al.*, Phys. Rev. B **50**, 17 383 (1995).
- ²⁶D. G. Polyakov and K. V. Samokhin, Phys. Rev. Lett. **80**, 1509 (1998).
- ²⁷B. L. Al'tshuler, A. G. Aronov, and D. E. Khmel'nitskii, J. Phys. C **15**, 7367 (1982); W. Eiler, J. Low Temp. Phys. **56**, 481 (1984).
- ²⁸D. B. Chklovskii, B. I. Shklovskii, and L. I. Glazman, Phys. Rev. B **46**, 4026 (1992).
- ²⁹A. A. Koulakov, M. M. Fogler, and B. I. Shklovskii, Phys. Rev. Lett. **76**, 499 (1996).
- ³⁰M. P. A. Fisher, G. Grinstein, and S. M. Girvin, Phys. Rev. B **40**, 587 (1989).
- ³¹L. W. Engel, D. Shahar, C. Kurdak, and D. C. Tsui, Phys. Rev. Lett. **71**, 2638 (1993).